corrosion and materials degradation

MDPI

Article

Preliminary Assessment of Cooling Water Chemistry for Fusion Power Plants

Eugenio Lo Piccolo [1], Raffaele Torella [1], Nicholas Terranova [2], Luigi Di Pace [2,*], Claudia Gasparrini [3,4] and Mauro Dalla Palma [3]

[1] RINA Consulting-Centro Sviluppo Materiali S.p.A. Roma, Via di Castel Romano 100, 00128 Rome, Italy; eugenio.lopiccolo@rina.org (E.L.P.); raffaele.torella@rina.org (R.T.)
[2] ENEA Fusion and Technology for Nuclear Safety and Security Department, CR Frascati, Via Enrico Fermi 45, 00044 Frascati, Italy; nicholas.terranova@enea.it
[3] Consorzio RFX (CNR, ENEA, INFN, Università di Padova, Acciaierie Venete S.p.A.), 35127 Padova, Italy; claudia.gasparrini@igi.cnr.it or c.gasparrini14@imperial.ac.uk (C.G.); mauro.dallapalma@igi.cnr.it (M.D.P.)
[4] Department of Materials & Centre for Nuclear Engineering, Imperial College London, London SW7 2AZ, UK
* Correspondence: dipace.luigi@gmail.com

Abstract: The determination of the water chemistry for cooling systems of nuclear fusion plants is under debate. It should be tailored for different types of fusion reactors: either experimental, e.g., ITER, JT-60SA, and DTT, or aimed at power generation, e.g., DEMO, given the different operation requirements. This paper presents the dual approach involving experiments and computer simulations chosen for the definition of DEMO water chemistry. Experimental work was performed to assess the corrosion susceptibility of reduced activation ferritic martensitic EUROFER 97 and AISI 316L in different water chemistry regimes. At the same time, the low corrosivity requirement brings an additional safety aspect for the radiation protection since some neutron-activated corrosion products (ACPs) create a gamma radiation when deposited outside the plasma chamber in components accessible to operators and these must be minimized. To evaluate the ACP inventory for DEMO, assessments were carried out using a reference computer code. Preliminary experimental activities to define the water chemistry of DTT under construction at ENEA were also conducted. The comparison of code results with experiments is two-fold important: for the validation of the computer code models and to determine data that are necessary to perform calculations.

Keywords: water chemistry; ACPs; RAFM EUROFER 97; fusion reactor cooling system; DEMO; DTT

check for updates

Citation: Lo Piccolo, E.; Torella, R.; Terranova, N.; Di Pace, L.; Gasparrini, C.; Dalla Palma, M. Preliminary Assessment of Cooling Water Chemistry for Fusion Power Plants. *Corros. Mater. Degrad.* **2021**, *1*, 1–19. https://doi.org/

Academic Editor: Raman Singh

Received: 22 June 2021
Accepted: 26 August 2021
Published:

Publisher's Note: MDPI stays neutral with regard to jurisdictional claims in published maps and institutional affiliations.

Copyright: © 2021 by the authors. Licensee MDPI, Basel, Switzerland. This article is an open access article distributed under the terms and conditions of the Creative Commons Attribution (CC BY) license (https://creativecommons.org/licenses/by/4.0/).

1. Introduction

The determination of a suitable water chemistry to be used for the cooling system of nuclear fusion plants is still under debate [1–3]. The complexity of this task is related to the different requirements needed for each experimental fusion reactor under construction, for ITER [4] (International Thermonuclear Experimental Reactor), and for DTT [5] (Divertor Tokamak Test) or in commissioning such as JT-60SA [6] (JT60 Super Advanced) as well as those in the design stage aimed to demonstrate power generation such as DEMO [7]. Fusion power reactors operate in either steady state (e.g., DEMO) or in pulsed mode (ITER, JT-60SA and DTT), where an alternation between oxidizing and reducing conditions is foreseen. This operation has a drastic effect on water chemistry since the pulsed mode induces an oxidizing environment due to the effects of gamma and neutron irradiation on water radiolysis [8]. The oxidizing environment during the pulse is then alternated to a reducing environment, which is preferable for both copper alloys and stainless steels. Power plant operation using a reducing environment has been implemented for decades in pressurized water reactors (PWRs), for example, where this is obtained through hydrogen injection in the range of 25 to 35 $cm^3\,kg^{-1}$ [9].

Corrosion and erosion phenomena play an important role in mobilizing activated materials in nuclear fusion machines [10–12]. When corrosion occurs in stainless steel, two different oxide layers are formed. The inner sublayer is a chromium-rich spinel that is adherent to the base metal. The surface layer is loosely adherent, and it is characterized by large iron-rich tetrahedral crystals (deposits), which agglomerate through precipitation processes of ions and particles transported by the cooling fluid.

The primary coolant transports ions generated by corrosion/release phenomena and oxide dissolution. When it is supersaturated in corrosion products, ions can precipitate to form wall deposits or particles suspended in the cooling fluid. Corrosion products in terms of ions in solutions, clusters, and deposits may encounter intense neutron flux in nuclear fusion applications. High-energy neutrons induce transmutation reactions, generating unstable nuclei, which can constitute a radiological hazard. Activated corrosion products (ACPs) in Primary Heat Transfer Systems (PHTSs) are significant sources of radiological hazard in nuclear reactors. Predicting transport of contaminants in a nuclear reactor cooling circuit may provide benefits in terms of radiation exposure assessment and mitigation, operation optimization, waste management, and hazardous source term identification [2,8,13,14].

Several computer codes have been developed over the years to monitor ACPs in nuclear applications (e.g., PACTOLE [1], TRACT [15], PACTITER [16], OSCAR [17], and CATE [13], among others), and they have been used to scan different technical and operational solutions devoted to decreasing the general corrosion of structural and piping materials. Minimizing general corrosion has the dual aim of reducing the outage time in case of corrosion induced failures and the dose to operators in charge of maintenance and inspections. It is well known that ACPs are responsible for the largest fraction of occupational doses in PWRs, especially during shutdown when corrosion increases due to the ingress of oxygen in the cooling circuits [18].

The main aim of the work is to present the preliminary experimental activity for the definition of water chemistry for DEMO through autoclave and loop tests performed to assess corrosion susceptibility of Reduced Activation Ferritic-Martensitic (RAFM) EUROFER 97 and AISI 316L steels used for the plasma chamber structure and piping materials. The presence of different materials (RAFM EUROFER 97 and copper alloys) in fusion reactors compared with PWRs is another element that adds complexity to this task. The optimization consisted of choosing a tailored water chemistry that ensures low corrosiveness, low impact in term of ACP generation, low neutron absorption to guarantee a suitable tritium production in the Breeder Blanket (BB), and suppression of radiolysis. Different water chemistry formulations were proposed, and preliminary autoclave testing was performed to evaluate the corrosion susceptibility of RAFM EUROFER 97 and AISI 316L base metals. Further tests on weld joints of EUROFER 97 and EUROFER 97-AISI 316L were carried out to investigate the effect of welding on corrosion performance. The water chemistry formulation tested so far considered the addition of LiOH and buffer NH_3. The results were promising, and first indications for an optimized cooling water chemistry are here presented.

The importance of validating computer codes with experimental tests is also highlighted. Experimental data obtained for EUROFER 97 have been used to validate the porosity parameters in PACTITER v2.1, which has been extensively used in support of the ITER Generic Site Safety Report (GSSR) and the ITER Preliminary Safety Report [19] for accident analyses and worker collective dose assessments and in preliminary ACP invenotory assessments for DEMO PHTS [14,20] .

Furthermore, preliminary experimental activities to define the water chemistry of DTT under construction at ENEA Frascati Research Centre (Italy) are briefly presented here. The DTT exploits the use of boric acid in the vacuum vessel (VV) cooling circuit as a nuclear shield.

2. Materials and Methods for Experimental Activities

2.1. Demo Wcll Water Chemistry Optimization

At RINA Consulting-Centro Sviluppo Materiali (RC-CSM), corrosion testings were performed using an autoclave equipped with a rotating sample holder system (see Figure 1) and an experimental corrosion loop, named HTHP (High Temperature High Pressure, see Figure 2). Both aimed to simulate the steady-state operative conditions of the breeding blanket of DEMO during plasma burning. Coolant and specimens were at a temperature of 300 °C. The systems were pressurized at 155 bar, simulating a flow rate of 2 m s^{-1}, with the typical coolant speed in the breeding blanket zone.

The exposure time was fixed at 1000 h. During this time interval, temperature, pressure, the HTHP flow rate, and the autoclave rotative speed were maintained constant. The water solutions were prepared in a laboratory using ultrapure compounds. Their deareation was performed by pure nitrogen tailoring an oxygen contamination lower than 10 ppb.

To perform autoclave testing, a 20 L apparatus equipped with a sample stirring (shown in Figure 1) was used. The speciemens were placed into a rotative cage, and the rotation speed was set at 150 rpm to simulate a DEMO water speed of 2 m s^{-1}. The pressure conditions were achieved using pure nitrogen.

In the HTHP testing procedure, tank B (see Figure 2) was used as a storage and loading tank of ultra-pure water (UPW). The test vessel A was loaded thanks to a nitrogen feed, which was also used for loop de-aeration and purging. Once the loop was loaded and pressurized, the nitrogen inlet was closed and the high-pressure circulating pump was activated. A heating system acting on tank A allowed us to reproduce high temperature conditions. A third tank C was used for water dumping and sampling.

Two typologies of speciemens for the corrosion test program were prepared: flat coupons and U-bend speciemens. The flat coupons were the following:

- EUROFER 97 coupons (Type A),
- AISI 316L coupons (Type B),
- Heterogeneous welded joints constituted by EUROFER 97 and AISI 316L with a central welded zone (Type AB), and
- Homogeneous welded joints constituted by EUROFER 97 with a central welded zone (Type AA).

On the other hand, the U-bend specimens were only made of AISI 316L and Ni-Alloy UNS625. The material fabrication method was performed at the RC-CSM steelwork plant according to the following steps:

- A primary production phase of Vacuum Induction Melting (VIM),
- A Vacuum Arc Remelting (VAR) for the second phase, and
- A final melting in a prismatic ingot of 80 kg.

EUROFER ingots hot rolling was realized by the RC-CSM rolling plant to produce plates with a wall thickness of 5 mm. The chemical composition of the EUROFER-97 steel sheets produced at RC-CSM is shown in the following Table 1.

Table 1. Chemical composition (wt %) of the EUROFER-97 plate material (Fe balanced).

Cr	Ni	Mn	Ti	V	Al	Ta	W	Mo
8.89	0.01	0.51	0.005	0.34	0.01	0.10	0.92	0.01
C	Si	P	Sn	Sb	N	S	Co	Nb
0.11	0.05	0.005	0.001	0.001	0.21	0.003	0.06	0.01

The final heat treatments applied after the rolling process were normalization at 980 °C for about 30 min and tempering at 760 °C for 90 min, both followed by air-cooling.

The AISI 316L was a commercial product coming from a hot rolling process with a final annealing treatment. Annealing was accomplished by heating in the 1040 to 1175 °C temperature range followed by air cooling or a water quench. Cooling should be sufficiently rapid (between 816 and 427 °C) to avoid reprecipitation of chromium carbides and to provide optimum corrosion resistance.

The Ni-Alloy UNS625 was a forged bar (6 in of diameter). The heat treatment consisted of stabilizing annealing at temperatures of 1093–1204 °C. Water quenching should be carried out rapidly to achieve optimal corrosion characteristics.

The welded joints were obtained using a TIG process [21] in two passes using a single V-edge of preparation. A Post Weld Heat Treatment (PWHT) at 760 °C for 2 h was also performed.

The water chemistry considered for testing was characterized by buffer solutions of 0.5 to 8.0 ppm of LiOH, 500 to 750 ppm of NH_3, and 5 $cm^3\,kg^{-1}$ of H_2 for radiolysis suppression. In PWRs, it was found that 5 $cm^3\,kg^{-1}$ of H_2 was enough to suppress the water radiolysis [22].

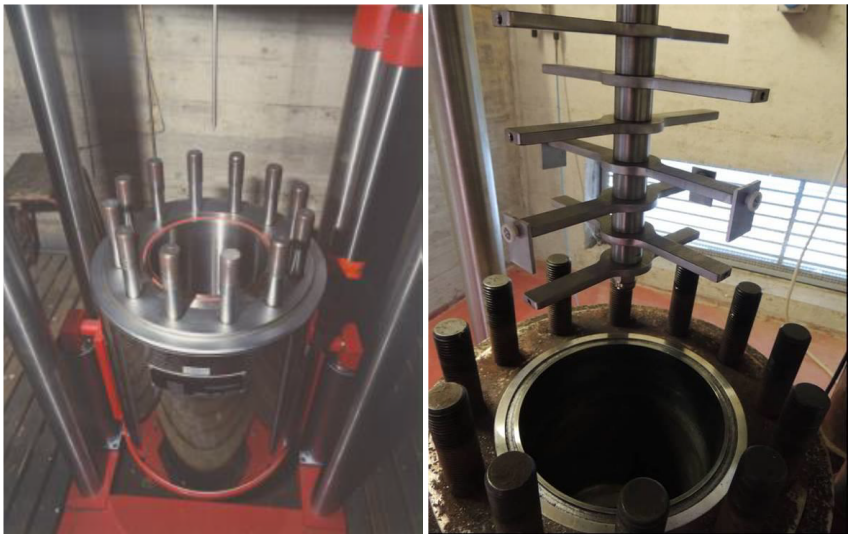


Figure 1. Autoclave (20 L) for corrosion testing with the water stirring apparatus.

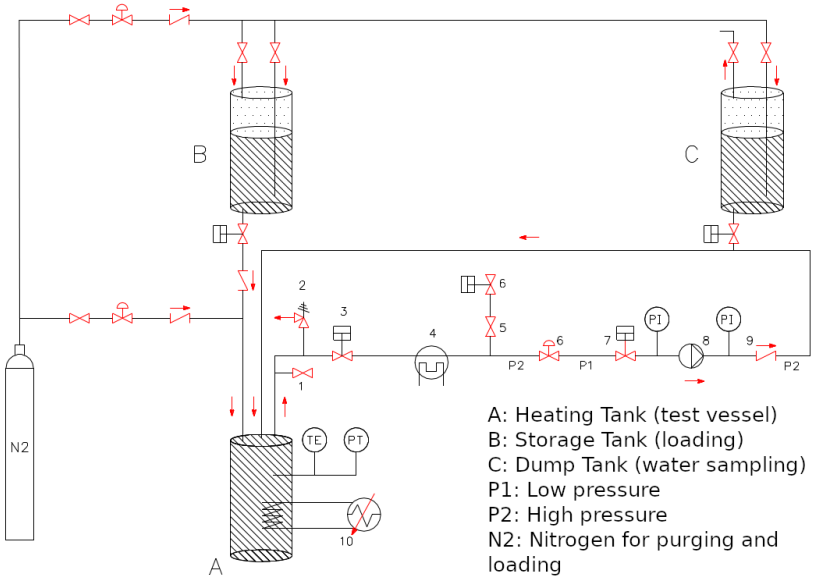


Figure 2. Layout of the HTHP corrosion testing loop. The test vessel (A) capacity was 2 L.

For the analysis of the specimens after corrosion testing, the following main tools were used:

- Scanning Electron Miscroscope (SEM) Model Zeiss EVO MA-15;
- Transmission Electron Microscopy (TEM), Model JEOL JEM-3200FS-HR, for the characterization of the oxide scale forms; and
- Focussed Ion Beam milling combined with Scanning Electron Microscopy (FIB-SEM) for the extraction of the TEM lamella from the sample top surface.

2.2. DTT VV Water Cooling Circuit Chemistry

Usually, pH in PWRs is kept under control within 6.9 to 7.4 at 300 °C [9,23]. This is possible thanks to the addition of chemicals that keeps the pH at room temperature (25 °C) within $pH_{25°C}$ = 6.2–7.3. The main additive used in western PWRs is LiOH (enriched with 99.9 wt % in ^{7}Li to minimize tritium production) with Li varying within 0.5 to 4 ppm. The addition of LiOH in PWRs' primary water is used to neutralize the pH of borated water containing 0 to 2400 ppm of B [23,24] during reactor operation.

Borated water in PWRs is used mostly as a reactivity control agent. The use of borated water in fusion reactors JT-60SA and DTT has, instead, the primary function of shielding the superconducting coils via neutrons generated in the tokamak plasma during fusion reactions. In this case, borated water has to be highly enriched in ^{10}B since this has a high neutron absorption cross section, approximately 0.2 barn at 1 MeV. ^{10}B absorbs neutrons through the $^{10}B(n, \alpha)^{7}Li$ reaction [25].

A first preliminary assessment for DTT VV water cooling circuit chemistry was performed using POTHY [26], the water chemistry subroutine of PACTITER v2.1. Water pH and AISI 316L alloying elements solubility were simulated in the temperature interval of interest for a DTT VV circuit between 40 and 80 °C.

The solubility of the main elements present in AISI 316L steel—Fe, Ni, Co, Cr, and Mn—were compared across three environments: UPW, borated water, and borated water stabilised by LiOH. The borated water contained 8000 ppm of boron since this is the upper requirement for DTT VV during high-performance plasma tests [27]. UPW was simulated considering no LiOH addition and with 0.1 ppm of B and H_2 as this is the minimum concentration possible in POTHY. The water chemistry simulated agreed well with the theoretical UPW behavior [28]. A simplified scheme of a loop was simulated in PACTITER v2.1 to evaluate the release and deposit of corrosion products from a stainless steel surface exposed to several borated water solutions. The loop design, based on the CORELE circuit [16], did not have filtering capabilities, and the only surface that was allowed to interact with the cooling media was a steel AISI 316L pipe. The pipe surface area was 0.314 m^2, the fluid velocity was 1 $m\,s^{-1}$,d the temperature of the media was T = 200 °C, and the initial thickness of the deposit in the pipe was 10^{-10} $mg\,cm^{-2}$.

To validate whether the chemistry code simulated the borated water environment well, complimentary experiments were performed. The water pH estimated by the code was compared with the experimental one. The 8000 ppm borated water was made by adding H_3BO_3 (4.58 wt %) from Borax (Optibor EP, 20 Mule Team, Rio Tinto, Borax Europe Limited, London, UK) to UPW (conductivity of 0.055 $\mu S\,cm^{-1}$ at 25 °C produced by an in-house purification system at Consorzio RFX, Padua, Italy). The measurement of pH with temperature was performed using a Testo 206 pHmeter. The solution was kept in a plastic beaker and stirred with a PTFE magnetic stirrer. The beaker was sealed with parafilm to avoid evaporation and was placed on a hot plate. The pH measurements were taken after the solution stabilised at the set temperature. To ensure that temperature measurements were correct, a second thermocouple was submerged in the solution.

3. Results

3.1. Results of Experimental Activities for DEMO WCLL BB Water Chemistry

Post-examination was performed using the following techniques:

- The form of the corrosion (uniform or localized) in both EUROFER 97 and welded specimens was determined using a 3D optical microscope (OM);
- The presence of cracks originated by Stress Corrosion Cracking (SCC) phenomena was investigated through OM observations on cross-sectioned U-bended speciemens (only on AISI 316L and Ni alloy 625 in autoclave);
- SEM and Energy Dispersion Spectroscopy (EDS) analyses on cross-sectioned specimens; and
- TEM and EDS analyses on cross sectioned specimens to evaluate the oxide layer composition, structure, and porosity.

Corrosion rates were calculated according to two different wight loss procedures:

- The first one considers the initial and the final weights of the coupons, without any corrosion product removal from the surfaces.
- The second approach compares the speciemens weight after a gentle chemical pickling with specific acid solutions in order to evalute oxide scale formation during exposure. The removal was performed in accordance with the ASTM G1 procedure.

A summary of the corrosion testing results performed in autoclave related to LiOH water chemistry is reported in the following graphics shown in Figure 3. The first one, in Figure 3a, shows the correlation between the corrosion rate of EUROFER as a function of LiOH concentration, while the second one, Figure 3b, is a diagram of the iron concentration versus LiOH concentration. Finally, Figure 3c shows the correlation of the final water pH measured at room temperature as a function of LiOH concentration.

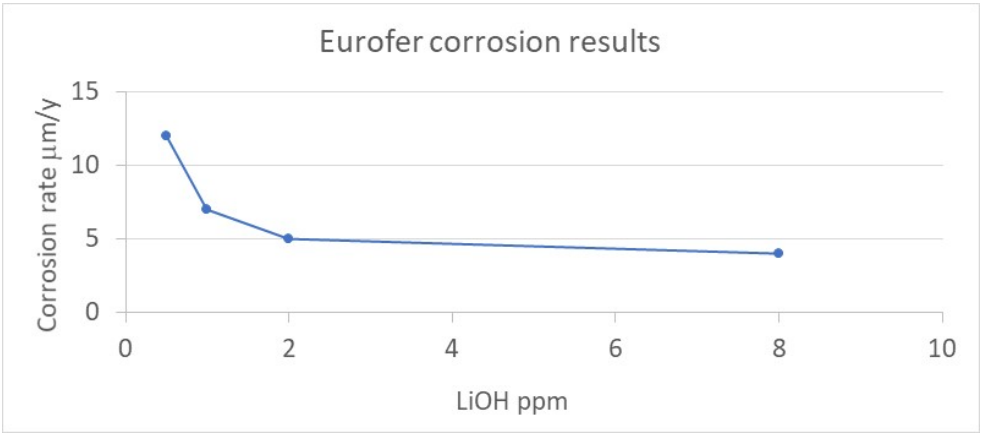
The corrosion rates of welded joint samples, which are not reported in the above graphics, showed higher values with respect to the unwelded samples. In general, the corrosion rates of welded samples are 30 to 50% higher than those of base material.

Furthermore, other tests were performed at the target pH 7.8 and 8.0 on Austenitic AISI 316L and Ni alloys 625 U-bend sample, to evaluate the risk of SCC phenomenon at high pH and high temperature. The results were very positive, and in all tests, the susceptibility to SCC was not detected. Concerning the corrosion rates of the EUROFER and AISI 316L in ammonia water chemistry, a summary of the main results is shown in Table 2 below.

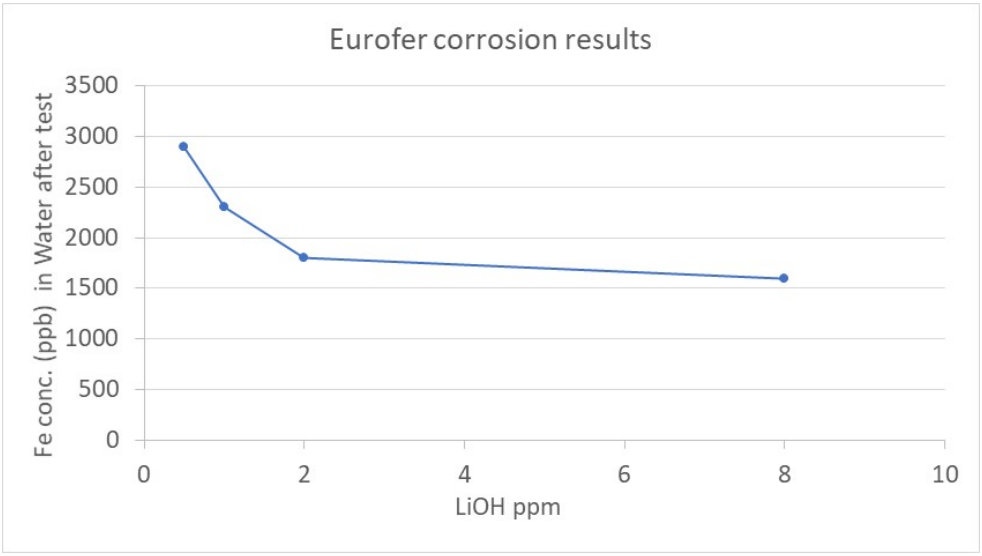
Table 2. Corrosion rates of EUROFER and AISI 316L in ammonia water chemistry.

NH_3 Concentration (ppm)	**EUROFER Corrosion Rate ($\mu m\, yr^{-1}$)**	**AISI 316L Corrosion Rate ($\mu m\, yr^{-1}$)**
500	5	1
750	4	1

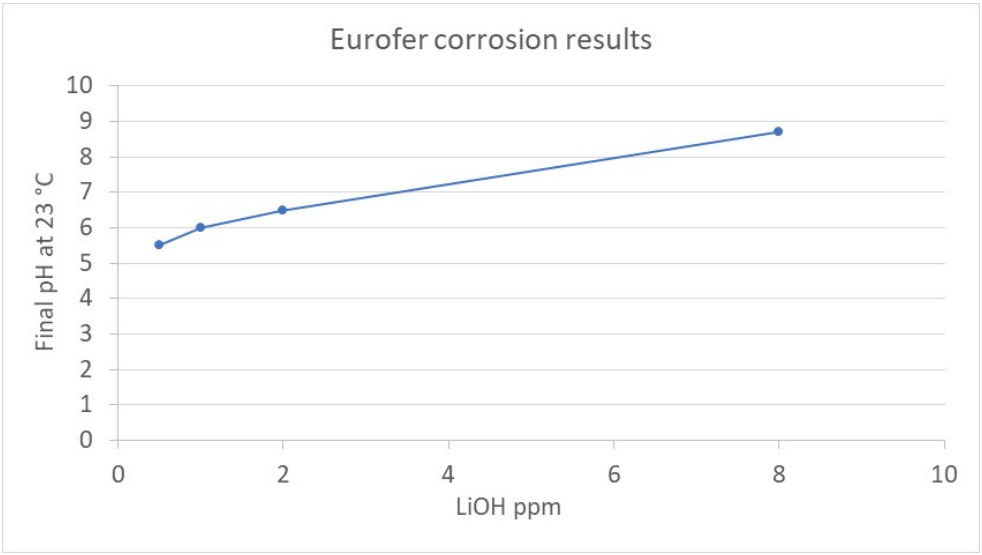
To simulate the corrosion behavior of EUROFER 97 and AISI 316L, some material properties are needed as input in PACTITER v2.1. One of the inputs needed is EUROFER 97 oxide porosity. An oxide porosity of approximately 40% (percentage of the area populated by pores with respect to the total area) was considered as input data for ACP evaluation in PACTITER v2.1 (see in the following). A specific post-test analysis of oxide scale was performed. The selected sample for this analysis was EUROFER 97 exposed to a water solution buffered with 500 ppm of NH_3 for 1000 h. The characterization of the oxide scale was carried out by TEM, and the extraction of the TEM lamella was obtained by FIB-SEM; see Figure 4 below.



(**a**)



(**b**)



(**c**)

Figure 3. Summary of the EUROFER corrosion results performed in autoclave and corrosion loop (HTHP) facilities: (**a**) EUROFER corrosion rate as a function of LiOH concentration. Corrosion rate data were calculated on the base of weight loss measurements, according to the ASTM G1 procedure. (**b**) Diagram of the iron concentration versus LiOH concentration. (**c**) Correlation of the final water pH measured at RT as a function of LiOH concentration.

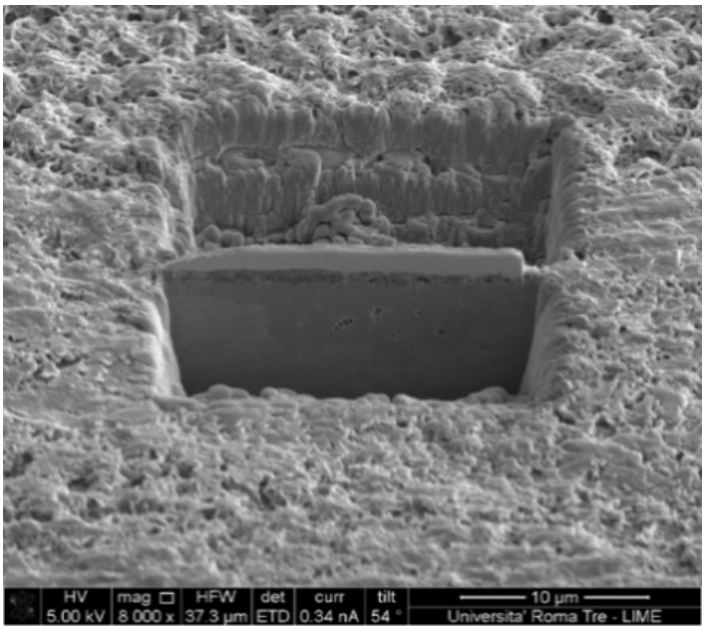


Figure 4. Three-dimensional image of a thin sample during the phase of extraction by FIB-SEM [29].

The image analysis by TEM allowed us to identify the porosity of the oxide scale. Figure 5 shows the morphology of the typical porous observed on a cross section of EUROFER oxide.

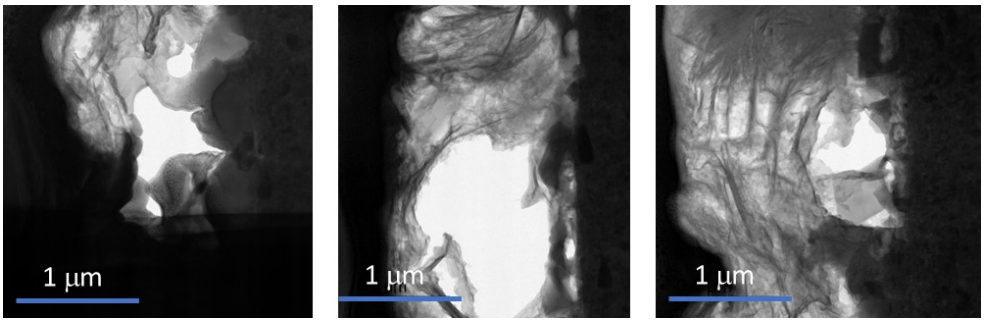


Figure 5. The figure shows the morphology of the pores observed on a cross section on the EUROFER oxide scale by TEM in bright field (BF) mode [29].

Eight different representative zones were examined by TEM for the evaluation of oxide porosity percentage. Table 3 presents the related values of this examination (the percentage average value was 10.3%, in a range 1.4 to 43%).

Table 3. Porosity for the eight representative zones after the corrosion test on EUROFER in a water solution buffered with 500 ppm of NH_3.

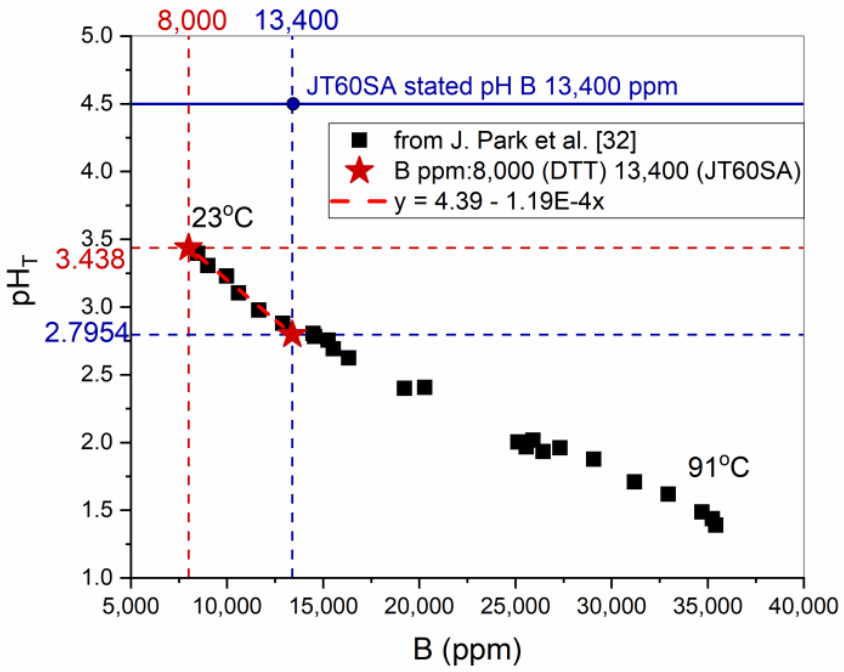
Zone	1	2	3	4	5	6	7	8	Total Ave.
%	1.4	43.0	6.3	8.6	1.8	2.8	7.9	11.1	10.3

The comparison with the PACTITER v2.1 results of the corrosion rate for DEMO WCLL First Wall (FW) PHTS is provided in Section 4.

3.2. Preliminary Activities for DTT VV Water Cooling Circuit Chemistry

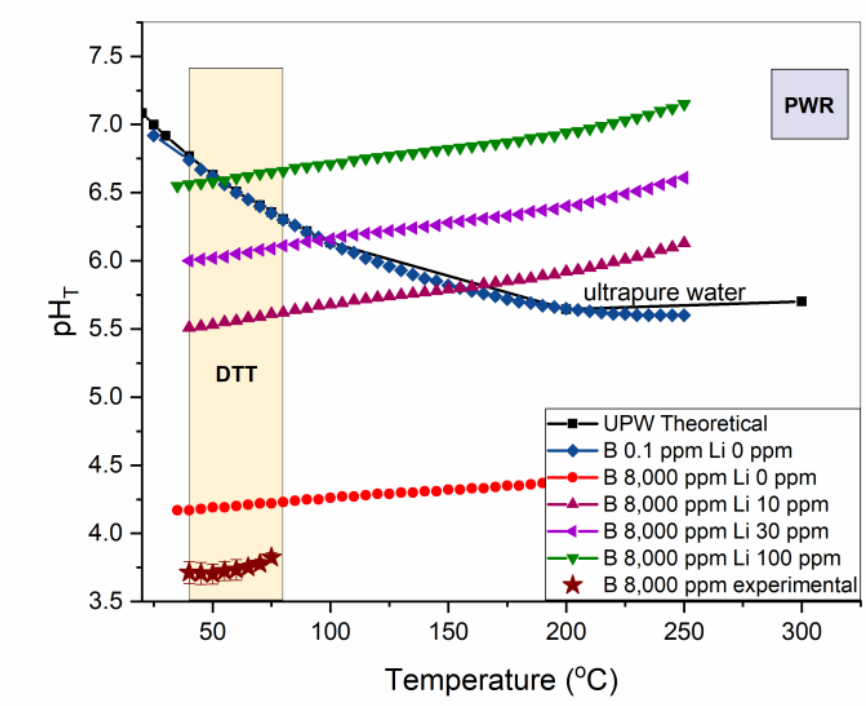
To understand the release of corrosion products in the DTT VV during alternating operations using UPW and borated water, both experiments and computer simulations were used. The POTHY chemistry subroutine of PACTITER v2.1 [26] simulated the water pH and solubility of the main elements of stainless-steel during corrosion processes.

The boric acid quantities needed in the DTT [30] and JT-60SA [31] fusion reactors are 8000 ppm and 13,400 ppm in B, respectively, which is well above the operational experience seen in PWRs. No additives are considered yet for the neutralization of borated water in the DTT VV cooling circuit; therefore, to choose the best water chemistry in this circuit, both modelling and experiments were used. Figure 6a shows the pH_T of borated water solutions at their saturation temperature, and the data were taken from J. Park et al. [32]. The pH_T of DTT and JT-60SA borated water solutions were extrapolated from the fitting of experimental data between 8500 ppm and 14,000 ppm; the fitting is shown with a dashed line [32] in Figure 6a. The pH_T of a solution with 8000 ppm B was estimated to be 3.44, whilst the pH_T of a 13,400 ppm B was 2.80. These values are shown by markers in Figure 6a. The stated pH_T of 13,400 ppm B solution in the JT-60SA Plant integration document was, however, pH = 4.5, very different from the fitted experimental pH_T in Figure 6a. To the best of our knowledge, no decision has been made yet on the additives to be used in JT-60SA VV cooling circuit.



(**a**)

Figure 6. *Cont.*



(**b**)

Figure 6. pH$_T$ as a function of temperature for borated solutions: (**a**) experimental data of pH$_T$ with temperature for a borated saturated solution taken from [32], the estimated pH$_T$ of borated water for DTT (8000 ppm B) and JT60SA (13,400 ppm B) are highlighted with a star. (**b**) pH$_T$ with the temperature of UPW and a borated water solution simulated with POTHY software; experimental data obtained for a 8000 ppm B solution are shown with a star (this study).

The measure of pH can be affected by the boric acid solubility with temperature; however, the pH measured experimentally in 8000 ppm B solutions in this study was similar to the one extrapolated from the data reported by J. Park et al. [32]. The experimental pH$_T$ values of a 8000 ppm B solution with temperature were plotted in Figure 6b: the pH$_T$ = 3.71 ± 0.08 at saturation. The simulated pH$_T$ of a borated water solution with 8000 ppm B in POTHY was higher: pH = 4.17 at 40 °C, as shown in Figure 6b. The software used to simulate borated water solutions seemed to overestimate the pH values with temperature, meaning a less aggressive solution is simulated by the code. The general trend of pH$_T$ with temperature is well represented by the software since an increase in pH with temperature is observed both from the model and from the experiments.

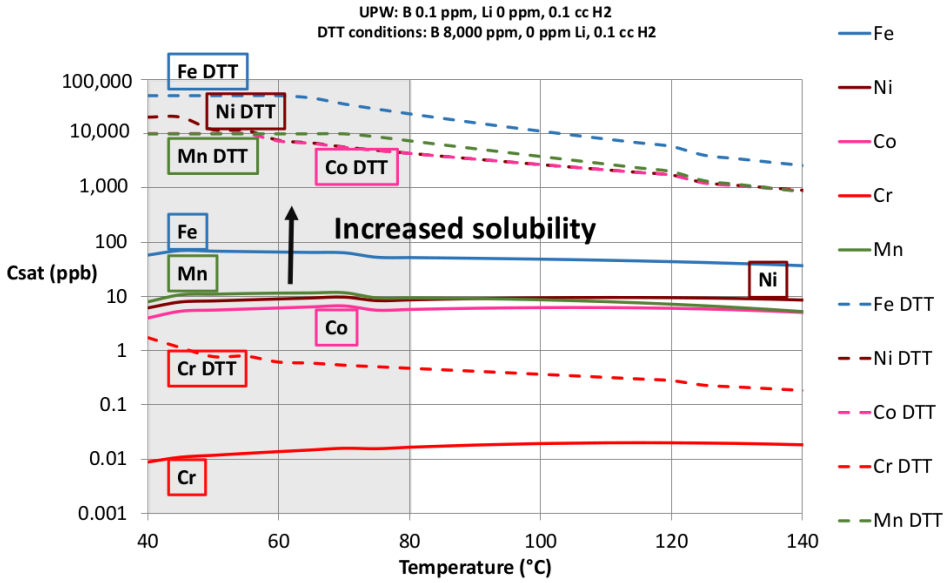
The use of a software has the advantage of testing several water chemistry regimes and enables a screening of the additives to be added to minimize the corrosive environment. The neutralization of boric acid in the DTT VV water circuit was simulated by the addition of LiOH. This relies on the 60+ years' experience of operation of PWRs from which the POTHY chemistry module was derived.

Figure 6b shows the pH$_T$ of borated water solutions (8000 ppm B) with the addition of 0, 10, 30, and 100 ppm of Li as LiOH. The DTT VV operating temperature is highlighted in yellow (T = 40–80 °C), whilst the operating temperature of PWRs (T = 288–316 °C) is highlighted in light blue (Figure 6b).

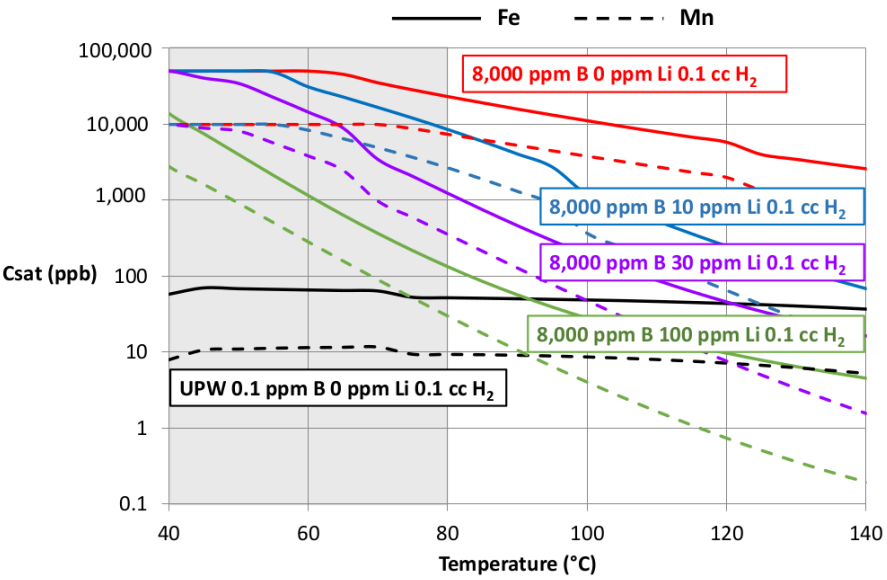
A comparison between pH$_T$ of borated water and UPW water with temperature enables us to compare the naturally acidic nature of UPW when heated to 250 °C. POTHY simulated the behavior of UPW well, since the pH = 5.65 at 200 °C (B 0.1 ppm, Li 0 ppm curve in Figure 6b) and the theoretical pH of UPW at 200 °C is 5.65 [28]. Having a pH of 5.5 in the cooling circuit is therefore acceptable (since UPW shows this behavior); furthermore, IAEA guidelines [33] suggest that a pH value between 4.5 and 7 should be a good compromise for metals exposed to 1 µS cm^{-1} water.

By keeping these guidelines in mind, the addition of 10 ppm of Li in 8000 ppm B water should be enough to maintain the pH of the solution at around 5.5. The addition of higher quantities of LiOH in the water (Li > 4 ppm) may be detrimental since LiOH is considered responsible for phenomena such as SCC in Inconel and Zircaloy [34]. The conductivity of 8000 ppm B and 10 ppm Li water is well above the IAEA limit of 1 µS cm^{-1} water, but the temperature is lower than most reactor applications.

To understand the release of metals in the circuit and how these are affected by the addition of LiOH, the solubilities of Fe, Ni, Co, Cr, and Mn were simulated for each borated water solution; these are plotted in Figure 7a.



(**a**)

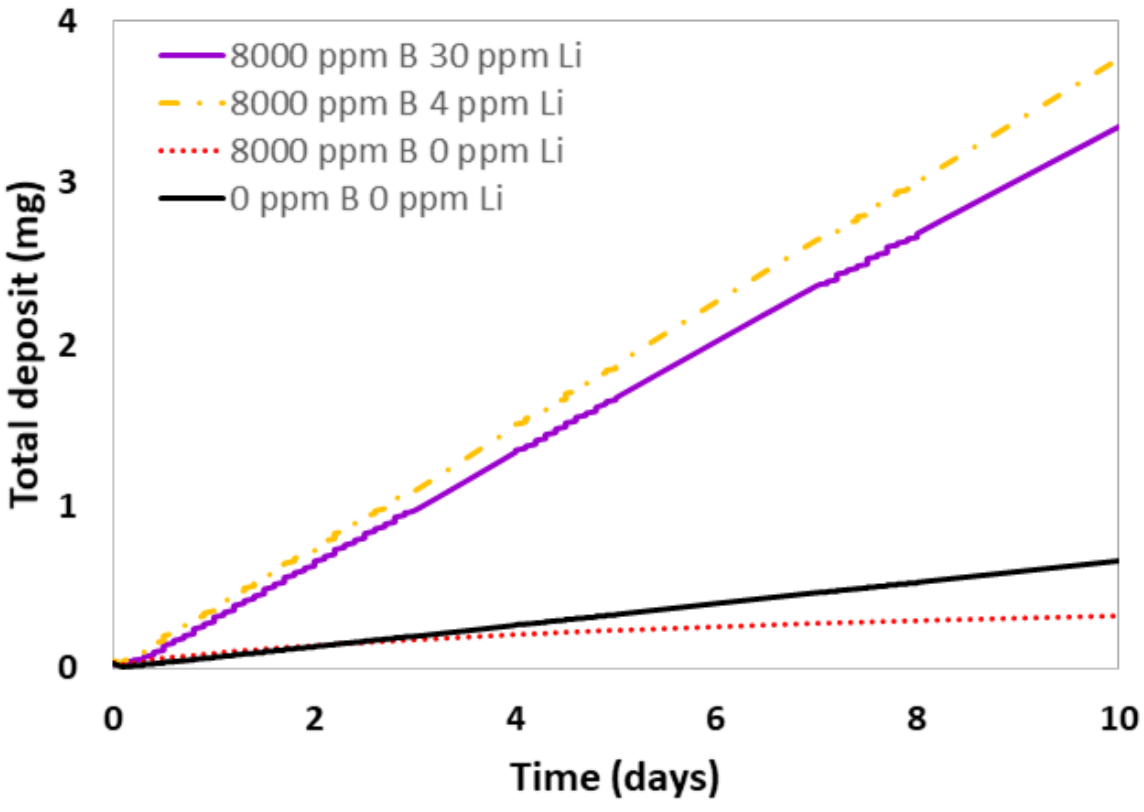


(**b**)

Figure 7. Solubility data obtained from POTHY: (**a**) the solubility of cations in a UPW environment (solid lines) vs. borated water (8000 ppm B) with no LiOH addition (dashed lines) to simulate DTT VV cooling circuit. (**b**) Comparison of the solubility of Fe (solid line) and Mn (dashed line) in the case of a borated water solution with the addition of 0, 10, 30, and 100 ppm Li as LiOH.

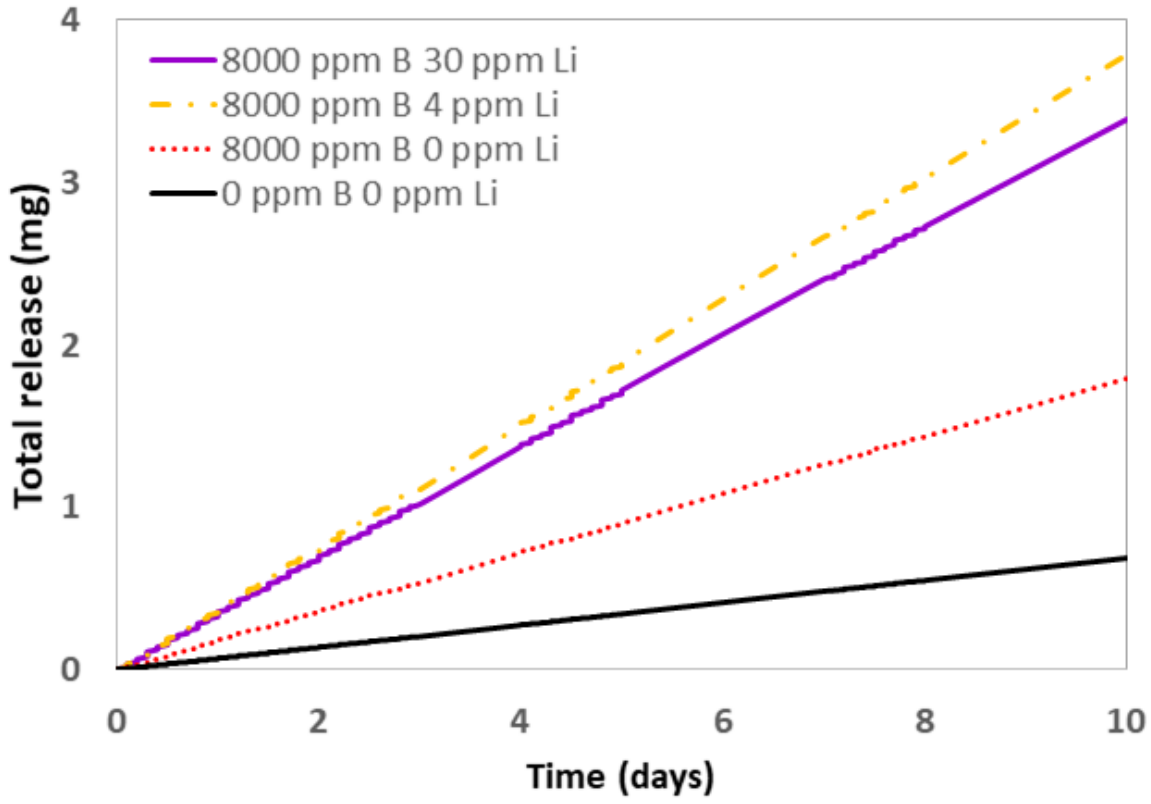
From Figure 7a, it is possible to observe that solubilities of Fe, Ni, Co, Cr, and Mn in the 40–80 °C temperature interval were three orders of magnitude larger in the borated water (with 8000 ppm B) solution compared with the use of UPW. Simulated solubilities of Fe and Mn change drastically above 60 °C; see Figure 7b. A slight improvement in terms of the Fe, Ni, Co, Cr, and Mn solubilities was observed in the borated water scenario (8000 ppm B) with the addition of 10 ppm Li compared with no addition of Li at 80 °C. To reduce drastically solubilities, a considerable amount of lithium, 100 ppm Li as LiOH, should be added. This cannot be realistically considered since 4 ppm Li is the safe upper limit in PWR water chemistry operations.

To assess whether the addition of LiOH would help minimize corrosion buildup, a simplified scheme based on the CORELE circuit [16] was used. As can be seen in Figure 8a,b, the stabilization of boric acid (8000 ppm B) with a base, LiOH, is not a straightforward solution for minimizing corrosion product build-up in the circuit. The loop was exposed to operations either in UPW or in borated water solutions (8000 ppm B) containing 0 ppm Li, 4 ppm Li, or 30 ppm Li for 10 days. Using 4 ppm Li as LiOH (PWR's upper limit concentration) did not mitigate the corrosion release process and mass deposit formation. The addition of 4 ppm Li was worse compared with the non-neutralization of the acid (0 ppm Li: dotted line). The neutralization with either 4 ppm Li or 30 ppm Li (bold line) showed a similar behavior in terms of corrosion product buildup and release.



(**a**)

Figure 8. *Cont.*



(**b**)

Figure 8. Surface of a stainless steel tube exposed to borated water solutions simulated using PACTITER 2.1 (elements considered are Fe, Ni, Mn, Co, and Cr): (**a**) total mass deposit and (**b**) metal release.

3.3. Comparison of Corrosion Experiments Results with Pactiter V2.1 Code Corrosion Rates Predictions

The outer oxide layer is characterized by an open porosity that allows for direct contact between the inner, more adherent, sublayer, and the cooling fluid. The growth of the deposits may limit the mass transfer between the inner oxide and the fluid, but ions can still be exchanged through corrosion/release mechanisms depending on the oxide morphology. In PACTITER v2.1, the release rate R_i for element i is calculated according to the following equation:

$$R_i = \frac{hDvZ_i}{Dz + h\sqrt{2x}}(C_{sat,i} - C_i) \quad (1)$$

where h is the ion transfer coefficient from the oxide surface to the coolant bulk, D is the coolant diffusion coefficient, v is the ratio between the open pore surface and the geometrical surface called POROS in PACTITER v2.1, Z_i is the element i content in the base metal, x is the deposit thickness, $C_{sat,i}$ is the equilibrium concentration (solubility) of element i at pipe wall, and C_i is the element concentration in the coolant bulk. In the calculations documented in [14], a conservative value of 0.4 (i.e., 40% of open oxide porosity) has been assumed for EUROFER 97 for the POROS parameter. To validate such a value for EUROFER 97, the corrosion and release rates evaluated using PACTITER v2.1 have been compared with the experimental results described above. Table 4 shows the corrosion rate measurements for 1000 h exposure of EUROFER specimens to a water solution of pH = 6.8 at 300 °C and 155 bar. Two samples were considered: EUROFER 97 (Type A) and a homogeneous welded joint EUROFER 97-EUROFER 97 (Type AA), showing corrosion rate values of 10.5 and 18 μm yr^{-1}, respectively.

Table 4. Corrosion rates measurements for 1000 h exposure at 300 °C, 155 bar, and 2 m s^{-1} for EUROFER specimens.

Solution pH	Specimen/Mat.	Corr. Rate μm yr^{-1}	Weight Loss mg m^{-2}
6.8 (1 ppm of LiOH)	Type A EUR_3	10.5	9.42
	Type AA EUR_3	18.0	16.15

Eight different representative zones of the EUROFER oxide layer were examined by TEM for the evaluation of the oxide porosity as already shown in Table 3.

The PACTITER v2.1 results on ACP assessment for DEMO-WCLL-FW-PHTS (in similar conditions with $pH_{300°C}$ = 7.0) have been analyzed to extrapolate corrosion rates as functions of time for both scenarios (pulsed and continuous). The corrosion rates of 48.6 μm yr^{-1} and 45 μm yr^{-1} have been determined after 1000 h of simulation time for the continuous and pulsed scenarios, respectively. The former value is compared with the experimental results in Table 4, related to steady-state conditions such as the simulated continuous scenario. The autoclave tests on specimens with average oxide porosity equal to about 10.3% (see Table 3), measured an average value for corrosion rate of 14.2 (10.5 + 18)/2 μm yr^{-1} (see Table 4). The ratio between the porosity and the corrosion rate for the experiments is 7.3 × 10^{-3} (0.103/14.2), and the same ratio calculated for PACTITER v2.1 simulation is 8.9 × 10^{-3} (0.4/45). This shows that, despite the differences between the two situations, there is a good agreement between the calculation hypotheses and the experiments and confirms that the choice made for calculations via PACTITER v2.1 about the POROS parameter for EUROFER 97, for which there was little or nothing of bibliographic evidence, was correct though rather conservative. Considering that OSCAR-Fusion v1.3 uses a completely different release and corrosion model from PACTITER v2.1, the role of experiments becomes fundamental for two reasons:

- To use validated input data, especially for EUROFER 97, for simulations runs;
- To validate not only corrosion and release models but also other main phenomena in ACP assessment by computer codes, transport, diffusion etc.

4. Discussion

4.1. Experimental Activities on DEMO WCLL BB Corrosion

The determination of a suitable cooling water chemistry for DEMO has to ensure low corrosivity, low impact in terms of ACPs generation, low neutron absorption, adequate tritium production, and suppression of radiolysis at temperatures around 280–320 °C.

The results obtained in this work showed that, moving toward pH values higher than 7.4, the LiOH concentration can have beneficial effects on corrosion rate. Such an advantage can be summarized as follows: the coolant showed more stable pH for a longer time near the neutral zone, which is the best condition for having passivity state of EUROFER 97, as described in the Pourbaix diagram pH–electrochemical potential [35]. Therefore, a less corrosive coolant can be achieved when reducing the ion and crude concentration in the PHTS circuit and when reducing the Chemical and Volume Control System (CVCS) adjustment and purification of the coolant during the life of the plant. At the same time, CVCS has to guarantee the set water chemistry parameters.

Another aspect considered is the maximum value of iron concentration in the coolant, which is an indication of the release capacity of the ACP for EUROFER and depends on the passive layer of magnetite. Different results were obtained when EUROFER 97 samples were tested in a first case before the formation of the magnetite layer and in a second case after its formation. After the formation of the magnetite layer, the test results showed that a plateau of the iron concentration is reached with 500 h of the test exposure. In the DEMO plant, the presence of the CVCS system can modify both the iron concentrations and the pH of the coolant during operation. This fact makes it unlikely that the magnetite layer is also generated in the nuclear plant, as was observed in the HTHP testing loop (schematized in Figure 2), with the same trend. The risk is that the achievable levels of

Fe concentration and pH in the DEMO plant are very different and such that the natural protective layer of magnetite cannot form in the EUROFER piping, as in the experimental loop. This phenomenon could lead to considering that the loop corrosion test is not very conservative, so that, in the real plant, higher values of corrosion rate may be observable for EUROFER. Therefore, it would be necessary to perform future tests that better simulate the continuous and dynamic change of the parameters of the water chemistry in the loop system, with frequent changes of solution, just to delay the magnetite formation, as it should be in a real plant.

The SCC results clearly showed that no stress cracking was observed in austenitic and Ni alloy, as reported by some authors [29,36] in the literature, considering the B–Li system. In the Li regime, without the effect of B, the operative range of the pH is influenced only by the precipitation of the iron hydroxides [37,38], which quickly reduce the initial pH of the coolant. On the other hand, the water equilibrium is more complex in the B–Li regime and the neutronic transmutation of the ^{10}B in ^{7}Li and α emission must be considered a source of alkalization of the coolant. This fact can explain the reason why many others recommended maintaining the pH of the coolant between 6.8 and 7.4 when the B–Li regime is adopted, adding a few parts per million of LiOH, with a maximum of 4 ppm.

Another important aspect analyzed through the experiments was associated to the corrosion code PACTITER v2.1 adopted so far for DEMO ACP assessments. As reported in Section 3.3, the relationship providing the release rate from the base metal and hence driving the corrosion rate is the open oxide porosity (parameter ν) that is the ratio between the open pore surface and the geometrical surface (named POROS in PACTITER v2.1 input). Usually, the POROS value adopted for AISI 316L is around 0.04, supported by experiments and PWR experiences. As the first guess for EUROFER 97, also taking into account its lower resistance to corrosion, a value 10 times larger, i.e., 0.40, was conservatively assumed. The correlation with experiments was performed as described in Section 3.3. The oxide porosity was investigated by TEM analysis of cross sectioned specimen. The experimental average value of porosity and the EUROFER 97 corrosion rate were in good agreement with the corresponding values given by the code in the sense that these two parameters are in the same ratio. However, the distribution of porosity into the scale detected by TEM analysis showed a more complex scenario, as reported in Figure 5: in some part of the scale, the observed porosity was predominant, while in another minor zone, it was extremely low. Such a distribution could be caused by an acceleration of the corrosion processes that occurred in the first month of exposure, which generated anisotropies in the oxide film formation and therefore inhomogeneous distribution of the porosities through the oxide film.

4.2. Experimental Activities on DTT VV Water Cooling Circuit Chemistry

Neutron shielding function in DTT-VV is planned to be achieved with the addition of boric acid enriched up to 95% in the isotope ^{10}B [27,31,39] in quantities higher than that generally used in PWRs. The use of boric acid in the cooling circuit complicates the chemistry choice to be implemented to minimize corrosion product buildup. During normal operation, it is envisaged that high purity water is used, and 0.3 $\mu S\,cm^{-1}$ water is proposed to be used for JT60-SA [40]. Keeping a low conductivity water ensures small concentrations of contaminants and dissolved gases, such as oxygen, which minimizes SCC whilst maintaining a low Oxidation-Reduction Potential (ORP) [23]. Furthermore, using UPW [28], conductivity of 0.055 $\mu S\,cm^{-1}$ at 25 °C, as feedwater ensures minimal galvanic corrosion of metallic materials in the circuit.

Galvanic corrosion acts through a "long cell action corrosion mechanism" [41] and is minimized by low conductivity; this is important in fusion reactors since different materials, copper alloys and stainless steels, are present in the circuit.

The addition of 8000 ppm B in DTT increases the water conductivity greatly as well as affects the pH_T. PACTITER v2.1 overestimated the pH_T of 8000 ppm B solutions. Even though the pH definition is widely accepted since it depends on water dissociation

constants (Kw), there are several models that describe Kw and therefore the pH_T of water. POTHY pH_T is calculated based on the Mesmer and Baes [42] model: this was specifically chosen to best fit the pH_T measurements conducted by CEA up to 300 °C. POTHY was used to simulate the pH_T of solutions in the temperature interval 25 to 100 °C, where models for the pH of UPW are consistent with each other.

The discrepancies observed in the pH_T definition of 8000 ppm B solutions between POTHY and experimental data, as shown in Figure 6, may be therefore related to the complex chemistry of boric acid in water which would react according to

$$B(OH)_3 + 2\,H_2O = B(OH)_4^- + H_3O^+$$

The chemistry of boric acid in water is further complicated by the formation of polyborates anions [42,43].

For a solution with 8000 ppm B, a conductivity of approximately 40 $\mu S\,cm^{-1}$ at 80 °C and a pH_T = 3.44 [32] is expected compared with UPW = 0.455 $\mu S\,cm^{-1}$ at 80 °C and a pH_T = 6.3 [28]. This reduction in pH_T and increase in conductivity enhance the general corrosion of steels and galvanic corrosion in the DTT VV cooling circuit. To minimize corrosion processes, the addition LiOH was assessed using ACP codes. Even though the addition of Li showed a beneficial effect in terms of decreasing metals solubility in the borated water solutions simulated by POTHY (see Figure 7b) the release and deposit of corrosion products simulated by PACTITER 2.1 was minimized when no LiOH was added (see Figure 8). The addition of 30 ppm LiOH to neutralize pH_T did not help the contrasting corrosion of AISI 316L surfaces; furthermore, this quantity is above the concentrations currently used in PWRs. Experimental tests are therefore conducted to assess the corrosion of AISI 316L in 8000 ppm B solutions considering no addition or small quantities addition of LiOH.

4.3. Overall Discussion

Given the complexity of the task in defining the best water chemistry for each specific fusion reactor, a dual approach involving both computer simulations and experiments was retained, being decisive in obtaining successful results. The requirement of low corrosivity in the cooling systems of fusion plants has an important additional safety aspect from the point of view of radiation protection since some of the corrosion products are neutron-activated (ACPs). They are mainly generated in the plasma chamber structure (blanket and divertor) cooled by the refrigerant in the form of ions and particles transported and deposited onto the circuit in components accessible to operators, valves, piping, pumps, and a steam generator, creating a gamma radiation. In addition, ACPs also imply safety issues in the event of loss-of-coolant accidents (LOCA). The comparison of code results with experiments is two-fold important: on one hand, for the validation of the computer code models and, on the other hand, to determine parameters necessary to carry out computer simulations, such as corrosion and release rates from new materials (e.g., EUROFER 97) at unconventional conditions of temperatures and water chemistry, and the morphological characteristics of the oxides that form on their surfaces which control the corrosion mechanism. In this regard, a preliminary comparison of the experimental data for corrosion rates with the predictions of the code is presented and discussed. Hence, it is well recognized that the chemistry control of the primary circuit is one essential component of radiation protection optimization in fission nuclear power plants [44]. The same can be stated for fusion reactors adopting water as cooling media, even though tangible evidence does not exist, with most of the experimental fusion reactors not actively being cooled; the exceptions are JET, D-III-D, ASDEX, etc. From that stems the importance paid to studying the water chemistry to be used in the next experimental and power fusion reactors in advance. Last but not least, it is important to mention that, among the operational (non-safety) functions required of the CVCS of DEMO PHTSs [45], there are those related to inventory control and make-up plus chemical control. The design of the DEMO CVCS is based not only on the knowledge acquired in the PWRs field but also on ongoing studies for

the definition of water chemistry, such as those documented in this article, in combination with the inventory assessment of ion and particles concentration obtained by dedicated calculation codes.

5. Conclusions

The water chemistry optimization for DEMO WCLL and DTT VV cooling circuits was discussed here. The optimization required both computer simulations and experimental work to be carried out simultaneously given the complicated requirements of fusion power plants that use innovative materials in circuits exposed to operating conditions never experienced in other power plants before. The main conclusions are summarized here:

- The corrosion testing in water chemistries with LiOH addition showed, in general, low corrosion rates for EUROFER and no cracking for AISI 316L, both on base materials and welded joint samples. Considering the corrosion behavior of a Ni-Alloy UNS625 as reference, similar results were obtained in the case of ammonia chemistries.
- EUROFER was shown to be more affected by uniform corrosion for the effect of welding process. In this regard, corrosion rates detected in the case of EUROFER welded joint specimens were 30–50% higher than those of unwelded samples.
- The beneficial effect of a higher pH condition was observed for the corrosion susceptibility of EUROFER, and no SCC phenomena was detected for both AISI 316 and Ni-Alloy UNS625. These results are very promising for enlarging the operative range of pH for LiOH chemistry, simplifying the chemistry control of the coolant for CVCS units.
- DTT VV exploited a highly enriched borated water (8000 ppm B) solution alternated to UPW as a coolant. The choice of adding a base, LiOH, to neutralize the borated water pH was discussed here, but contradictory results from simulations were obtained.
- Experimental tests showed that the ACP codes developed for PWR water chemistry regimes ($pH_{25°C}$ = 6.2–7.3 with Li varying from 0.5 to 4 ppm and B varying from 0 to 2400 ppm) overestimated the pH_T of 8000 ppm B borated water solution needed for DTT.
- The choice of adding LiOH to a DTT VV borated water solution needs to be validated by experimental tests to ensure that the code that will be used to assess DTT ACPs is representative of the real situation as well as to minimize corrosion in the circuit.

Author Contributions: Introduction, L.D.P., N.T., and C.G.; Materials and Methods for Experimental Activities and Calculation Tools: Section 2.1, R.T. and E.L.P.; Section 2.2, C.G. and M.D.P.; Results: Section 3.1, R.T. and E.L.P.; Section 3.2, C.G.; Section 3.3, L.D.P. and N.T.; Discussion: Section 4.1, E.L.P. and R.T.; Section 4.2, C.G. Section 4.3, all. All authors have read and agreed to the published version of the manuscript.

Funding: This work has been carried out within the framework of the EUROfusion Consortium and has received funding from the Euratom research and training programme 2014–2018 and 2019–2020 under grant agreement No. 633053 for the part related to experimental activities for DEMO water chemistry, ACP assessment, and DTT water chemistry. The views and opinions expressed herein do not necessarily reflect those of the European Commission.

Institutional Review Board Statement: Not applicable.

Informed Consent Statement: Not applicable.

Data Availability Statement: The datasets generated and analysed in this study are available from the corresponding author on request.

Conflicts of Interest: The authors declare that they have no known competing financial interests or personal relationships that could have appeared to influence the work reported in this paper.

References

1. Belous, V.; Kalinin, G.; Lorenzetto, P.; Velikopolskiy, S. Assessment of the corrosion behaviour of structural materials in the water coolant of ITER. *J. Nucl. Mater.* **1998**, *258–263*, 351–356, https://doi.org/10.1016/S0022-3115(98)00272-4.
2. Harrington, C.; Baron-Wiechec, A.; Burrows, R.; Holmes, R.; Clark, R.; Walters, S.; Martin, T.; Springell, R.; Öijerholm, J.; Becker, R.; et al. Chemistry and corrosion research and development for the water cooling circuits of European DEMO. *Fusion Eng. Des.* **2019**, *146*, 478–481, https://doi.org/10.1016/j.fusengdes.2018.12.095.
3. Cavallini, C.; Dalla Palma, M.; Fellin, F.; Gasparrini, C.; Tinti, P.; Zamengo, A.; Zaupa, M. Investigation of corrosion-erosion phenomena in the primary cooling system of SPIDER. *Fusion Eng. Des.* **2021**, *166*, 112271, doi:10.1016/j.fusengdes.2021.112271.
4. Bigot, B. ITER assembly phase: Progress toward first plasma. *Fusion Eng. Des.* **2021**, *164*, 112207, doi:10.1016/j.fusengdes.2020.112207.
5. Crisanti, F.; Martone, R.; Mazzitelli, G.; Pizzuto, A. The DTT device: Guidelines of the operating program. *Fusion Eng. Des.* **2017**, *122*, 382–386, https://doi.org/10.1016/j.fusengdes.2017.06.006.
6. Ishida, S.; Barabaschi, P.; Kamada, Y. Overview of the JT-60SA project. *Nucl. Fusion* **2011**, *51*, 094018, doi:10.1088/0029-5515/51/9/094018.
7. Federici, G.; Bachmann, C.; Barucca, L.; Biel, W.; Boccaccini, L.; Brown, R.; Bustreo, C.; Ciattaglia, S.; Cismondi, F.; Coleman, M.; et al. DEMO design activity in Europe: Progress and updates. *Fusion Eng. Des.* **2018**, *136*, 729–741. https://doi.org/10.1016/j.fusengdes.2018.04.001.
8. Karditsas, P.J. Water radiolysis in fusion neutron environments. *Fusion Eng. Des.* **2011**, *86*, 2701–2704, doi:10.1016/j.fusengdes.2010.12.040.
9. Kawamura, H.; Hirano, H.; Katsumura, Y.; Uchida, S.; Mizuno, T.; Kitajima, H.; Tsuzuki, Y.; Terachi, T.; Nagase, M.; Usui, N.; et al. BWR water chemistry guidelines and PWR primary water chemistry guidelines in Japan—Purpose and technical background. *Nucl. Eng. Des.* **2016**, *309*, 161–174, https://doi.org/10.1016/j.nucengdes.2016.08.029.
10. Di Pace, L.; Tarabelli, D.; You, D. Development of the PACTITER code and its application to the assessment of the ITER divertor cooling loop corrosion products. *Fusion Technol.* **1998**, *34*, 733–737.
11. Kot, A. *Water and Water Treatment in Nuclear Power Plants*; IPST: Jerusalem, Israel, 1964.
12. Castelli, R. *Nuclear Corrosion Modelling. The Nature of CRUD*; Elsevier Inc.: Amsterdam, The Netherlands, 2009.
13. Li, L.; Zhang, J.; Song, W.; Fu, Y.; Xu, X.; Chen, Y. CATE: A code for activated corrosion products evaluation of water-cooled fusion reactor. *Fusion Eng. Des.* **2015**, *100*, 340–344, https://doi.org/10.1016/j.fusengdes.2015.06.193.
14. Terranova, N.; Di Pace, L. DEMO WCLL primary heat transfer system loops activated corrosion products assessment. *Fusion Eng. Des.* **2021**, *170*, 112456, https://doi.org/10.1016/j.fusengdes.2021.112456.
15. Karditsas, P.; Caloutsis, A. Corrosion and activation in fusion cooling loops–TRACT. *Fusion Eng. Des.* **2007**, *82*, 2729–2733, https://doi.org/10.1016/j.fusengdes.2007.03.025.
16. Di Pace, L.; Dacquait, F.; Schindler, P.; Blet, V.; Nguyen, F.; Philibert, Y.; Larat, B. Development of the PACTITER code and its application to safety analyses of ITER Primary Cooling Water System. *Fusion Eng. Des.* **2007**, *82*, 237–247, https://doi.org/10.1016/j.fusengdes.2006.11.002.
17. Genin, J.; Marteau, H.; Dacquait, F. The OSCAR code package: A unique tool for simulating PWR contamination. In Proceedings of the Nuclear Power Plant Conference 2010 (NPC 2010): International Conference on Water Chemistry of Nuclear Reactor Systems and 8th International Radiolysis, Electrochemistry and Materials Performance Workshop, Quebec City, QC, Canada, 3–8 October 2010.
18. OECD/NEA. Occupational Exposures at Nuclear Power Plants. In *Twenty-Eighth Annual Report of the ISOE Programme*; Technical Report, No. 7536; NEA: Boulogne-Billancourt, France, 2021.
19. ITER. *Preliminary Safety Report (RPrS)*; Technical Report, IDM UID 3ZR2NC; ITER: Saint-Paul-lez-Durance, France, 2010.
20. Di Pace, L.; Quintieri, L. Assessment of activated corrosion products for the DEMO WCLL. *Fusion Eng. Des.* **2018**, *136*, 1168–1172, https://doi.org/10.1016/j.fusengdes.2018.04.095.
21. Welding and allied processes. Types of joint preparation. Part 1: Manual metal arc welding, gas-shielded metal arc welding, gas welding, TIG welding and beam welding of steels; EN ISO 9692-1:2013; The International Organization for Standardization: Geneva, Switzerland, 2013.
22. Christensen, H. Remodeling of the Oxidant Species During Radiolysis of High-Temperature Water in a Pressurized Water Reactor. *Nucl. Technol.* **1995**, *109*, 373–382, doi:10.13182/NT95-A35086.
23. Aaltonen, P.; Hanninen, H. *Water Chemistry and Behavior of Materials in PWRs and BWRs*; Technical Report, IAEA-TECDOC-965; IAEA: Vienna, Austria, 1997.
24. EPRI. *PWR Primary Water Chemistry Guidelines*; Technical Report; EPRI: Palo Alto, CA, USA, 2014.
25. Bevilacqua, R.; Hambsch, F.J.; Vidali, M.; Ruskov, I.; Lamia, L. ^{10}B(n, α)^{7}Li and ^{10}B(n,α1γ)^{7}Li cross section data up to 3 MeV incident neutron energy. *EPJ Web Conf.* **2017**, *146*, 11010, doi:10.1051/epjconf/201714611010.
26. Beslu, P. *PACTOLE: A Calculation Code for Predicting Corrosion Product Behavior and Activation in PWR Primary Coolant Systems*; Technical Report, CEA Technical Note SCOS-LCC-90-096; CEA: Saint-Paul-lez-Durance, France, 1990.
27. Martone, R.; Albanese, R.; Crisanti, F.; Pizzuto, A.; Martin, P. Divertor Tokamak Test Facility Interim Design Report. Available online: https://www.dtt-dms.enea.it/share/s/avvglhVQT2aSkSgV9vuEtw (accessed 22 June 2019).
28. Light, T.S. Temperature dependence and measurement of resistivity of pure water. *Anal. Chem.* **1984**, *56*, 1138–1142, doi:10.1021/ac00271a019.

29. Torella, R.; Lo Piccolo, E. *Water Chemistry Control: Validation of Buffered Water Solutions for WCLL BB System by Corrosion Testing*; Technical Report, WPBB 3.3.1 T005-D001 EFDA_D_2P5N82; EUROfusion: Garching, Germany, 2019.
30. Colangeli, A.; Villari, R.; Luis, R.; Moro, F.; Sandri, S.; Fonnesu, N.; Flammini, D.; Mariano, G.; Crisanti, F.; Ramogida, G.; et al. Neutronics study for DTT tokamak building. *Fusion Eng. Des.* **2019**, *146*, 2581–2585, https://doi.org/10.1016/j.fusengdes.2019.04.047.
31. Villari, R.; Barabaschi, P.; Cucchiaro, A.; della Corte, A.; Di Zenobio, A.; Dolgetta, N.; Lacroix, B.; Moro, F.; Muzzi, L.; Nicollet, S.; et al. Neutronic analysis of the JT-60SA toroidal magnets. *Fusion Eng. Des.* **2009**, *84*, 1947–1952, https://doi.org/10.1016/j.fusengdes.2009.01.035.
32. Park, J.H. *Boric Acid Corrosion of Light Water Reactor Pressure Vessel Materials*; Technical Report, NUREG/CR-6875; ANL: Washington, DC, USA, 2005.
33. IAEA. *Good Practices for Water Quality Management in Research Reactors and Spent Fuel Storage Facilities*; Technical Report, Nuclear Energy Series No. NP-T-5.2; IAEA: Vienna, Austria, 2011.
34. IAEA. *Coolant Technology of Water Cooled Reactors: An Overview*; Technical Report Series No. 347; IAEA: Vienna, Austria, 1993.
35. Pourbaix, M. *Atlas of Electrochemical Equilibria in Aqueous Solutions*; CEBELCOR: Brussels, Belgium, 1974.
36. EPRI. *PWR Primary Water Chemistry Guidelines*; Technical Report, TR-105714-V1R4; EPRI: Palo Alto, CA, USA, 1999.
37. Burrows, R.; Harrington, C.; Baron-Wiechec, A.; Warren, A. Warren A. Development of Conceptual Water Chemistry Guidelines for Water Coolant Circuits of a Demonstration Fusion Power Reactor. In Proceedings of the 20th Nuclear Plant Chemistry Conference, Brighton, UK, 2–7 October 2016.
38. Burrows, R.; Holmes, R.; Walters, S. *WPBB 3.3.2-T001-D002 EFDA_D_2NBJRL*; Technical Report; EUROfusion: Garching, Germany, 2018.
39. Villari, R.; Angelone, M.; Caiffi, B.; Colangeli, A.; Crisanti, F.; Flammini, D.; Fonnesu, N.; Luis, R.; Mariano, G.; Marocco, D.; et al. Nuclear design of Divertor Tokamak Test (DTT) facility. *Fusion Eng. Des.* **2020**, *155*, 111551, https://doi.org/10.1016/j.fusengdes.2020.111551.
40. Wanner, M. *Project Plant Integration Document (PID) V4.2*; Technical Report, JT-60 SA, BA_D_222UJY; JT-60 SA: Naka, Japan, 2020.
41. Saji, G. Degradation of aged plants by corrosion: "Long cell action" in unresolved corrosion issues. *Nucl. Eng. Des.* **2009**, *239*, 1591–1613.
42. Mesmer, R.E.; Baes, C.F.; Sweeton, F.H. Acidity measurements at elevated temperatures. IV. Apparent dissociation product of water in 1 m potassium chloride up to 292.deg. *J. Phys. Chem.* **1970**, *74*, 1937–1942, doi:10.1021/j100704a019.
43. Palmer, D.; Benezeth, P.; Wesolowski, D.J. Boric acid hydrolysis: A new look at the available data. Power Plant Chemistry. *Power Plant Chem.* **2000**, *2*, 261–264.
44. Provens, H. *Primary Circuit Contamination in Nuclear Power Plants: Contribution to Occupational Exposure*; Technical Report, Nucléaire; Institut de Radioprotection et de Sûreté: Fontenay aux Roses, France, 2002.
45. Garrone, E.; Caramello, M.; Paoletti, F.; Pierantoni, V. *Preliminary Concept Design Study of Cvcs for Demo Wcll Bb Phts&Bop Indirect Coupling Plan*; Technical Report; EUROfusion: Garching, Germany, 2020.